

Superconductivity at 28.3 K and 17.1 K in (Ca₄Al₂O_{6-y})(Fe₂Pn₂) (Pn = As and P)

Parasharam M. Shirage¹, Kunihiro Kihou^{1,2}, Chul-Ho Lee^{1,2}, Hijiri Kito^{1,2}, Hiroshi Eisaki^{1,2} and Akira Iyo^{1,2}

¹National Institute of Advanced Industrial Science and Technology, Tsukuba, Ibaraki 305-8568, Japan

²JST, Transformative Research-Project on Iron Pnictides (TRIP), 5, Sanbancho, Chiyoda, Tokyo 102-0075, Japan

Abstract: We have successfully synthesized (Ca₄Al₂O_{6-y})(Fe₂Pn₂) (Pn = As and P) (Al-42622(Pn)) using high-pressure synthesis technique. Al-42622(Pn) exhibit superconductivity for both Pn = As and P with the transition temperatures of 28.3 K and 17.1 K, respectively. The *a*-lattice parameters of Al-42622(Pn) (*a* = 3.713 Å and 3.692 Å for Pn = As and P, respectively) are smallest among the iron-pnictide superconductors. Correspondingly, Al-42622(As) has the smallest As-Fe-As bond angle (102.1 °) and the largest As distance from the Fe planes (1.500 Å).

PACS number(s):74.70.Dd, 74.62.Bf, 74.25.F-,74.10.+v

One of the salient features of the newly-discovered iron (Fe)-based superconductors is their wide material variation. Their basic crystal structure is an alternative stacking of the $FePn$ ($Pn=P, As$) layers sandwiched by the blocking layers. Variety of crystal structures can be realized by employing different blocking layers, such as LnO ($Ln=rare\ earth$)[1], Ae ($Ae=Ba, Sr, Ca, Eu$)[2], and A ($A=Li, Na$) [3]. Most recent achievement is the discovery of superconductors possessing perovskite-type blocking layers, $(Sr_4Sc_2O_6)(Fe_2P_2)$ [4], $(Sr_4M_2O_{6-y})(Fe_2As_2)$ ($M = V$ [5] and $MgTi$ [6]), $(Sr_4M_3O_8)(Fe_2As_2)$ ($M = ScTi$), $(Ba_4Sc_3O_{7.5})(Fe_2As_2)$ [7], $(Ca_{n+m}(M,Ti)_nO_y)(Fe_2As_2)$ ($M = Sc$ [8], Mg [9,10] and Al [11], $n = 2, 3, 4$ and 5 , $m = 1, 2$), with T_c reaching as high as 47 K for $(Ca_4(Mg,Ti)_3O_y)(Fe_2As_2)$. Another interesting feature is the strong correlation between their superconducting transition temperature (T_c) and the configuration of the $FeAs_4$ local structure, such as the $Pn-Fe-Pn$ bond angle (α) and/or the height of Pn atoms relative to the neighboring Fe layers (h_{Pn})[12, 13] and many theories have been proposed to account for the correlation [14, 15]. Considering these situations, synthesis of materials possessing either (1) new type of blocking layers or (2) unachieved $FeAs_4$ configurations, should be tremendously beneficial for understanding the high- T_c mechanism, and, eventually, for enhancing T_c , of the Fe-based superconductors.

Based on the above background, in this study we have attempted to synthesize new $FePn$ superconductors using a high-pressure (HP) technique. HP technique is established as a versatile tool to explore new materials beyond the limitation of ambient synthesis conditions [16]. By enforcing the stacking between the $FeAs$ layers and the blocking layers with smaller in-plane unit cell length (a -lattice parameters), this method allows us to synthesize materials with extremely smaller unit cell volumes. For example, we have succeeded in synthesizing a series of $LnFeAsO_{1-y}$

superconductors ($Ln=La, Ce, Pr, Nd, Sm, Gd, Tb, Dy$) that possess small Ln atoms, which yield small LnO blocking layers [17]. The unit cell volume largely shrinks from 141 \AA^3 ($Ln = La$) to as small as 124 \AA^3 ($Ln = Dy$). In this study, we have applied the HP technique in synthesizing new materials containing perovskite-type blocking layers which are extremely small and therefore cannot be synthesized under ambient conditions. Along this line, we have discovered a series of new $(Ca_4Al_2O_{6-y})(Fe_2Pn_2)$ ($Pn = As$ and P) (abbreviated as Al-42622(Pn)) superconductors with $T_c = 28.3$ K and 17.1 K, respectively. As a consequence of HP synthesis, the synthesized compounds possess the unique structural characteristics never realized in the existing Fe-based superconductors, namely, shortest a -axis lattice parameters, smallest As-Fe-As bond angle, and longest As-Fe plane distance. Here we demonstrate the synthesis method and the characterization of Al-42622(Pn).

Polycrystalline samples of Al-42622(Pn) were synthesized by the solid-state reaction method using a cubic-anvil-type HP apparatus. It should be noted that one cannot synthesize Al-42622(Pn) by conventional ambient pressure synthesis [11]. Starting materials were powders of CaO, Al, As, P, Fe and Fe_2O_3 . The powders were mixed with a nominal composition of $(Ca_4Al_2O_{6-y})(Fe_2Pn_2)$. Here the oxygen content $6-y$ was controlled by adjusting the ratio of Fe and Fe_2O_3 . We have found that the purity of the obtained samples strongly depends on the oxygen content in the starting composition. The suitable oxygen content turned out to be $6 - y = 5.6 \sim 5.8$. The starting materials were ground using an agate mortar and pressed into a pellet in a glove box filled with N_2 gas. The pellet was loaded in a high-pressure cell and heated at 1150 and 1300 °C for $Pn = As$ and P , respectively, under a pressure of 4.5 GPa for 1 h.

Powder X-ray diffraction (XRD) patterns were measured using CuK_α radiation.

Neutron scattering measurement was carried out using the high-resolution powder diffractometer HERMES of the Institute for Materials Research, Tohoku University, installed at the JRR-3 reactor of JAEA in Japan. Incident neutron wavelength was fixed at 1.8484 Å using a Ge monochromator. The data were analyzed by the Rietveld method using the Rietan program. The dc magnetic susceptibility was measured using a SQUID magnetometer (Quantum Design MPMS) under a magnetic field of 5 Oe. The resistivity was measured by a four-probe method.

Fig. 1 represent the XRD patterns of Al-42622(*Pn*) samples with nominal compositions of (a) $\text{Ca}_4\text{Al}_2\text{O}_{5.65}\text{Fe}_2\text{As}_2$ and (b) $\text{Ca}_4\text{Al}_2\text{O}_{5.80}\text{Fe}_2\text{P}_2$, respectively. Major peaks can be indexed based on the tetragonal crystal structure with $a = 3.713$ Å and $c = 15.407$ Å for Al-42622(As) while with $a = 3.692$ Å and $c = 14.934$ Å for Al-42622(P). Small impurity phases of CaO, and FeAs were detected in the Al-42622(As) samples. Note that the a -lattice parameter of Al-42622(As) is significantly smaller than those of Fe-As related compounds containing Ca-based perovskite-derived blocking layers, such as $(\text{Ca}_4(\text{Mg},\text{Ti})_3\text{O}_y)(\text{Fe}_2\text{As}_2)$ ($a = 3.877$ Å, $T_c = 47$ K) [9] and $(\text{Ca}_5(\text{Mg},\text{Ti})_4\text{O}_y)(\text{Fe}_2\text{As}_2)$ ($a = 3.864$ Å, $T_c = 43$ K) [10]. The contraction of the a -lattice parameter is reasonable, considering the smaller ionic radius size of Al^{3+} ($R_{\text{Al}} = 0.535$ Å) compared to Mg^{2+} ($R_{\text{Mg}} = 0.720$ Å) and Ti^{4+} ($R_{\text{Ti}} = 0.605$ Å) [18]. Similarly, the a -lattice parameter of Al-42622(P) is much smaller compared to the iso-structure compound, $(\text{Sr}_4\text{Sc}_2\text{O}_6)(\text{Fe}_2\text{P}_2)$ ($a = 4.016$ Å, $T_c = 17$ K), which contains larger Sc^{3+} ($R_{\text{Sc}} = 0.745$ Å) . It is worth stressing that the a -parameters of Al-42622(*Pn*) are smallest among ever-reported Fe-based superconductors. For example, typical materials having short a -lattice parameter are FeSe ($a = 3.769$ Å, $T_c = 8$ K)[19], LiFeAs ($a = 3.7914$ Å, $T_c = 18$ K) [3], $(\text{Ca},\text{Na})\text{Fe}_2\text{As}_2$ ($a = 3.880$ Å, $T_c = 26$ K)[20] or DyFeAsO_{1-y} ($a = 3.820$ Å, $T_c = 43$ K)[17].

The c -lattice parameters of Al-42622(Pn) are also significantly smaller than those of iso-structural 42622(Pn), such as $(Sr_4M_2O_{6-y})(Fe_2As_2)$ ($c = 15.809$ Å for $M = Sc$, 15.683 Å for $M = Cr$ and 15.673 Å for $M = V$), [5, 21] due to the smaller ionic radii of Ca^{2+} ($R_{Ca} = 1.00$ Å) and Al^{3+} compared to those of Sr^{2+} ($R_{Sr} = 1.180$ Å), Sc^{3+} ($R_{Sc} = 0.745$ Å), Cr^{3+} ($R_{Cr} = 0.615$ Å) and V^{3+} ($R_V = 0.640$ Å). Small lattice parameters of Al-42622(Pn) naturally explains why these compounds are synthesized only by HP technique. It also demonstrates the usefulness of HP technique for synthesizing materials possessing extremely smaller unit cell volumes.

Fig. 2(a-b) shows the temperature (T) dependence of the zero-field-cooled (ZFC) and the field-cooled (FC) magnetic susceptibility (χ) for the (a) Al-42622(As) and (b) Al-42622(P) samples. As shown in the inset Fig. 2, the sample shows superconducting transition with their onset temperature ($T_c^{\chi-onset}$) at 26.8 K and 17.0 K for Al-42622(As) and Al-42622(P), respectively. The superconducting volume fraction estimated from χ (ZFC) at 5 K without demagnetizing field correction are 115 % for Al-42622(As) and 96 % for Al-42622(P), respectively, ensuring the bulk superconductivity. For Al-42622(As), the reversible region, where ZFC and FC magnetization curves overlap with each other, exists from $T_c^{\chi-onset}$ to 21.5 K, possibly due to the grain pinning mechanism. The reversible behavior is a unique feature of the FeAs-based superconductors which contain the thick perovskite-type blocking layers, suggesting high anisotropy of their superconducting properties. In contrast, the reversible region of Al-42622(P) is extremely limited. This contrast indicates the difference of the anisotropy between the two systems, possibly because the spacing between Fe layers is shorter for Al-42622(P) compared to Al-42622(As).

In Fig. 3 T -dependent resistivity (ρ) of (a) Al-42622(As) and (b) Al-42622(P) are shown. Metallic behavior ($d\rho/dT > 0$) can be seen in the all T -range. In particular, for

42622(As), no kink in the resistivity, a signature of antiferromagnetic/orthorhombic transition, is observed. Accordingly, we can conclude that the system is away from the parent phase which possesses long-range structural/magnetic order. As indicated in the inset of Fig. 3(a), a broadening of transition (or a two-step transition) is recognized. T -range where the resistive broadening occurs seems to coincide with the reversible region observed in the χ - T curve. It may suggest that the broadening results from the flux creep in the reversible region. In Al-42622(P), very high (one order higher than Al-42622(As)) normal state resistivity and broad superconducting transition were observed. This is partly due to the poor sintering of the samples. As indicated in the insets, $T_c^{\rho-onset}$, $T_c^{\rho-mid}$ and $T_c^{\rho=0}$ are 28.3, 27.0, 23.0 K for Al-42622(As) and 17.1, 15.6, 6.0 K for Al-42622(P), respectively.

Our data indicate that the Al-42622(Pn) systems have the shortest a -lattice parameters among all the Fe-based superconductors. One would naively expect that the shrinkage of the a -lattice parameters causes the elongation of the $FePn_4$ tetrahedra along the c -axis. It is indeed confirmed by the neutron powder diffraction on Al-42622(As). Table I show the atomic positions of Al-42622(As) determined by the Rietveld analysis of the neutron powder diffraction. The calculated Fe-As-Fe bond angle α is $102.1(1)^\circ$. This value is much smaller than those of any other Fe-pnictide superconductors. For example, α of the $LnFeAsO$ -based materials ranges from 113° ($Ln = La$, $T_c = 27$ K) to 108° ($Ln = Dy$, $T_c = 52$ K). Similarly, α of $(Ba,K)Fe_2As_2$ ($T_c = 38$ K) is 109° . α of $LiFeAs$ ($T_c = 18$ K) is rather smaller, but still 104° . As for those containing Ca-based perovskite-derived blocking layers, α ranges from 107° for $Ca_5(Mg,Ti)_4O_{11}Fe_2As_2$ [10] to 109° for $Ca_4(Sc,Ti)_3O_8Fe_2As_2$ [8], estimated from the relation between the a -lattice parameter and h_{Pn} in ref.[22]. Empirically it is pointed out that the highest T_c materials possess α close to 109.5° , an angle where the $FeAs_4$

tetrahedron forms the regular shape. The relatively lower T_c of 28.3 K for Al-42622(As) compared to other Ca-based perovskite counterparts with T_c 's reaching 47 K is likely due to the elongation of the FeAs₄ tetrahedron. It should be also remarked that the height of As atoms relative to the Fe layers (h_{pn}) is 1.500 Å, which is the highest value among the Fe-pnictide superconductors.

In contrast, T_c of 17 K for Al-42622(P) is much higher than most of the existing FeP-based superconductors, such as LaFePO ($T_c = 4$ K)[23], LiFeP ($T_c = 6$ K)[24], *etc.* The only material which exhibits comparable T_c is (Sr₄Sc₂O₆)(Fe₂As₂) (Sc-42622(P)), which shares the same crystal structure as Al-42622(P). Note that their a -lattice parameters are significantly different from each other, $a = 3.692$ Å for Al-42622(P) and $a = 4.016$ Å for Sc-42622(P), respectively. The fact that T_c does not change between these two systems suggests that T_c of the FeP-based superconductors is rather insensitive to the structural parameters, contrary to the FeAs-based counterpart. Another possibility is that T_c of the 42622(P) system takes its maximum value when the a -lattice parameter falls between 3.692 Å and 4.016 Å. In this regard, it is intriguing to synthesize an alloy of Al-42622(P) and Sc-42622(P) and check whether one can enhance its T_c .

In summary, we have utilized HP technique to synthesize (Ca₄Al₂O_{6-y})(Fe₂Pn₂) ($Pn = \text{As}$ and P), which exhibit superconductivity at 28.3 K and 17.1 K for $Pn = \text{As}$ and P , respectively. These materials possess the shortest a -lattice parameters, correspondingly the smallest α and the highest h_{pn} among the Fe-pnictide superconductors.

Acknowledgements: We thank Prof. H. Ogino and Dr. N. Takeshita for fruitful discussions. This work was supported by a Grant-in-Aid for Specially Promoted Research (20001004) from The Ministry of Education, Culture, Sports, Science and

Technology (MEXT).

References:

- [1] Y. Kamihara, T. Watanabe, M. Hirano, and H. Hosono, *J. Am. Chem. Soc.* **130**, 3296 (2008).
- [2] M. Rotter, M. Tegel, I. Schellenberg, W. Hermes, R. Pottgen, and D. Johrendt, *Phys. Rev. B* **78**, 020503 (2008).
- [3] J. H. Tapp, Z. Tang, B. Lv, K. Sasmal, B. Lorenz, P. C. W. Chu, and A. M. Guloy, *Phys. Rev. B* **78**, 60505(2008).
- [4] H. Ogino, Y. Matsumura, Y. Katsura, K. Ushiyama, S. Horii, K. Kishio, and J. Shimoyama, *Supercond. Sci. Technol.* **22**, 75008 (2009).
- [5] X. Zhu, F. Han, G. Mu, P. Cheng, B. Shen, B. Zeng, and H. H. Wen, *Phys. Rev. B* **79**, 220512 (2009).
- [6] S. Sato, H. Ogino, N. Kawaguchi, Y. Katsura, K. Kishio, J. Shimoyama, H. Kotegawa, and H. Tou, *Supercond. Sci. Technol.* **23**, 45001(2010).
- [7] N. Kawaguchi, H. Ogino, Y. Shimizu, K. Kishio, and J. Shimoyama, *Appl. Phys. Exp.* **3**, 63102(2010).
- [8] H. Ogino, S. Sato, K. Kishio, J. Shimoyama, T. Tohei, and Y. Ikuhara, arXiv:1006.2355.
- [9] H. Ogino, Y. Shimizu, K. Ushiyama, N. Kawaguchi, K. Kishio, and J. Shimoyama, *Appl. Phys. Exp.* **3**, 63103 (2010).
- [10] Y. Shimizu, H. Ogino, N. Kawaguchi, K. Kishio, J. Shimoyama, arXiv:1006.3769.
- [11] H. Ogino and J. Shimoyama, private communication.
- [12] C.H. Lee, A. Iyo, H. Eisaki, H. Kito, M. T. Fernandez-Diaz, T. Ito, K. Kihou, H. Matsuhata, M. Braden, and K. Yamada, *J. Phys. Soc. Jpn.* **77**, 083704 (2008).
- [13] J. Zhao, Q. Huang, C. d. I. Cruz, S. Li, J. W. Lynn, Y. Chen, M. A. Green, G. F. Chen, G. Li, Z. Li, J. L. Luo, N. L. Wang, and P. Dai, *Nature Materials* **7**, 953 (2008).

- [14] V. Vildosola, L. Pourovskii, R. Arita, S. Biermann, and A. Georges, *Phys. Rev. B* **78**, 064518 (2008).
- [15] K. Kuroki, H. Usui, S. Onari, R. Arita, and H. Aoki, *Phys. Rev. B* **79**, 224511 (2009); G. A. Sawatzky, I. S. Elfimov, J. van den Brink, and J. Zaanen, *Europhys. Lett.* **86**, 17006 (2009).
- [16] P. M. Shirage, K. Miyazawa, M. Ishikado, K. Kihou, C.H. Lee, N. Takeshita, H. Matsuhata, R. Kumai, Y. Tomioka, T. Ito, H. Kito, H. Eisaki, S. Shamoto, and A. Iyo, *Physica C* **469**, 355 (2009).
- [17] K. Miyazawa, K. Kihou, P. M. Shirage, C. H. Lee, H. Kito, H. Eisaki, and A. Iyo, *J. Phys. Soc. Jpn.* **78**, 034712 (2009).
- [18] R. D. Shannon, *Acta Cryst. A* **32**, 751(1976).
- [19] F. C. Hsu, J. Y. Luo, K. W. Yeh, T. K. Chen, T. W. Huang, P. M. Wu, Y. C. Lee, Y. L. Huang, Y. Y. Chu, D. C. Yan, M. K. Wu, *Proc. Natl. Acad. Sci. USA*, **105**, 14262 (2008).
- [20] P. M. Shirage, K. Miyazawa, H. Kito, H. Eisaki, A. Iyo, *Appl. Phys. Exp.* **1**, 081702 (2008).
- [21] H. Ogino, Y. Katsura, S. Horii, K. Kishio, J. Shimoyama, *Supercond. Sci. Technol.* **22**, 85001 (2009).
- [22] H. Ogino, S. Sato, Y. Matsumura, N. Kawaguchi, K. Ushiyama, Y. Katsura, S. Horii, K. Kishio, J. Shimoyama, arXiv:1006.2351.
- [23] Y. Kamihara, H. Hiramatsu, M. Hirano, R. Kawamura, H. Yanagi, T. Kamiya, and H. Hosono, *J. Am. Chem. Soc.* **128**, 10012(2006).
- [24] Z. Deng, X. C. Wang, Q. Q. Liu, S. J. Zhang, Y. X. Lv, J. L. Zhu, R. C. Yu and C. Q. Jin, *Europhys. Lett.* **87**, 37004 (2009).

Figure captions

Figs. 1 X-ray diffraction patterns of (a) $\text{Ca}_4\text{Al}_2\text{O}_{6-y}\text{Fe}_2\text{As}_2$ and (b) $\text{Ca}_4\text{Al}_2\text{O}_{6-y}\text{Fe}_2\text{P}_2$ samples.

Figs. 2 Temperature (T) dependence of susceptibility (χ) of (a) $\text{Ca}_4\text{Al}_2\text{O}_{6-y}\text{Fe}_2\text{As}_2$ and (b) $\text{Ca}_4\text{Al}_2\text{O}_{6-y}\text{Fe}_2\text{P}_2$ samples. Data near the superconducting transitions. $T_c^{\chi\text{-onset}}$ is determined from the intersection of the two extrapolated lines; one is drawn through χ in the normal state just above T_c , and the other is drawn through the steepest part of χ in the superconducting state.

Figs. 3 T -dependence of resistivity (ρ) of (a) $\text{Ca}_4\text{Al}_2\text{O}_{6-y}\text{Fe}_2\text{As}_2$ and (b) $\text{Ca}_4\text{Al}_2\text{O}_{6-y}\text{Fe}_2\text{P}_2$ samples. Data near the superconducting transitions and a determination of T_c are shown in the insets. $T_c^{\rho\text{-onset}}$ is determined from the intersection of the two lines; one is drawn through ρ in the normal state just above T_c , and the other is drawn through the steepest part of ρ in the superconducting state. $T_c^{\rho\text{-mid}}$ is 50 % drop of $T_c^{\rho\text{-onset}}$ and $T_c^{\rho=0}$ is zero resistivity.

Table I. Atomic parameters of Al-42622(As) (space group $P4/nmm$) determined by a Rietveld refinement of neutron powder diffraction data at room temperature. B is the isotropic atomic displacement parameter. The lattice parameters are $a = 3.7133(1)$ Å and $c = 15.4035(6)$ Å. The R -factor is $R_{wp} = 5.261$.

Atom	site	x	y	z	B (Å ²)
Fe	2a	3/4	1/4	0.0	0.47(5)
As	2c	1/4	1/4	0.0974(2)	0.66(8)
Ca(1)	2c	1/4	1/4	0.7997(3)	0.18(9)
Ca(2)	2c	1/4	1/4	0.5819(3)	0.33(11)
Al	2c	1/4	1/4	0.3181(4)	0.50(14)
O(1)	4f	3/4	1/4	0.2969(2)	0.50(6)
O(2)	2c	1/4	1/4	0.4340(3)	0.69(9)

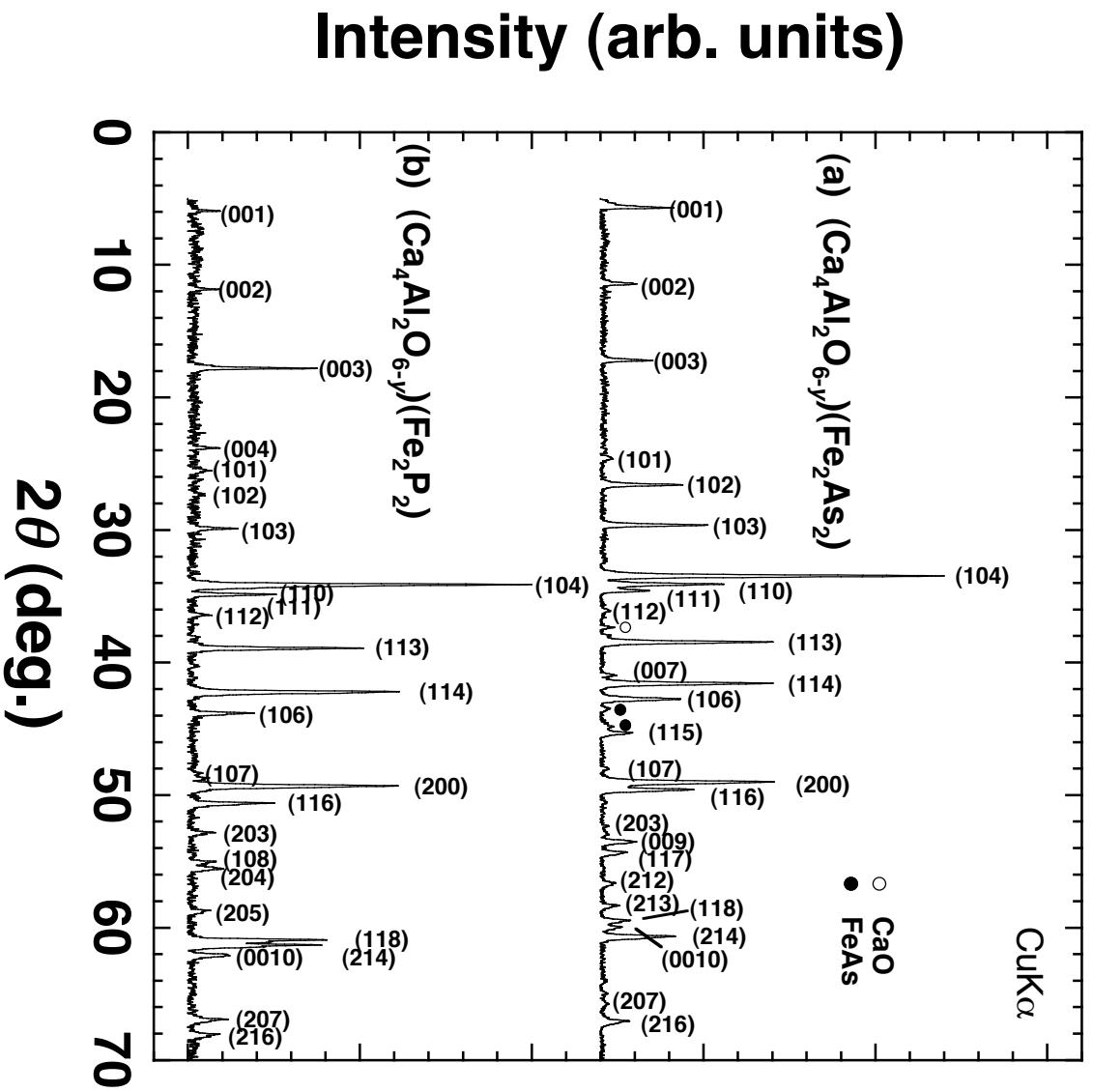


Figure 1 (a-b)

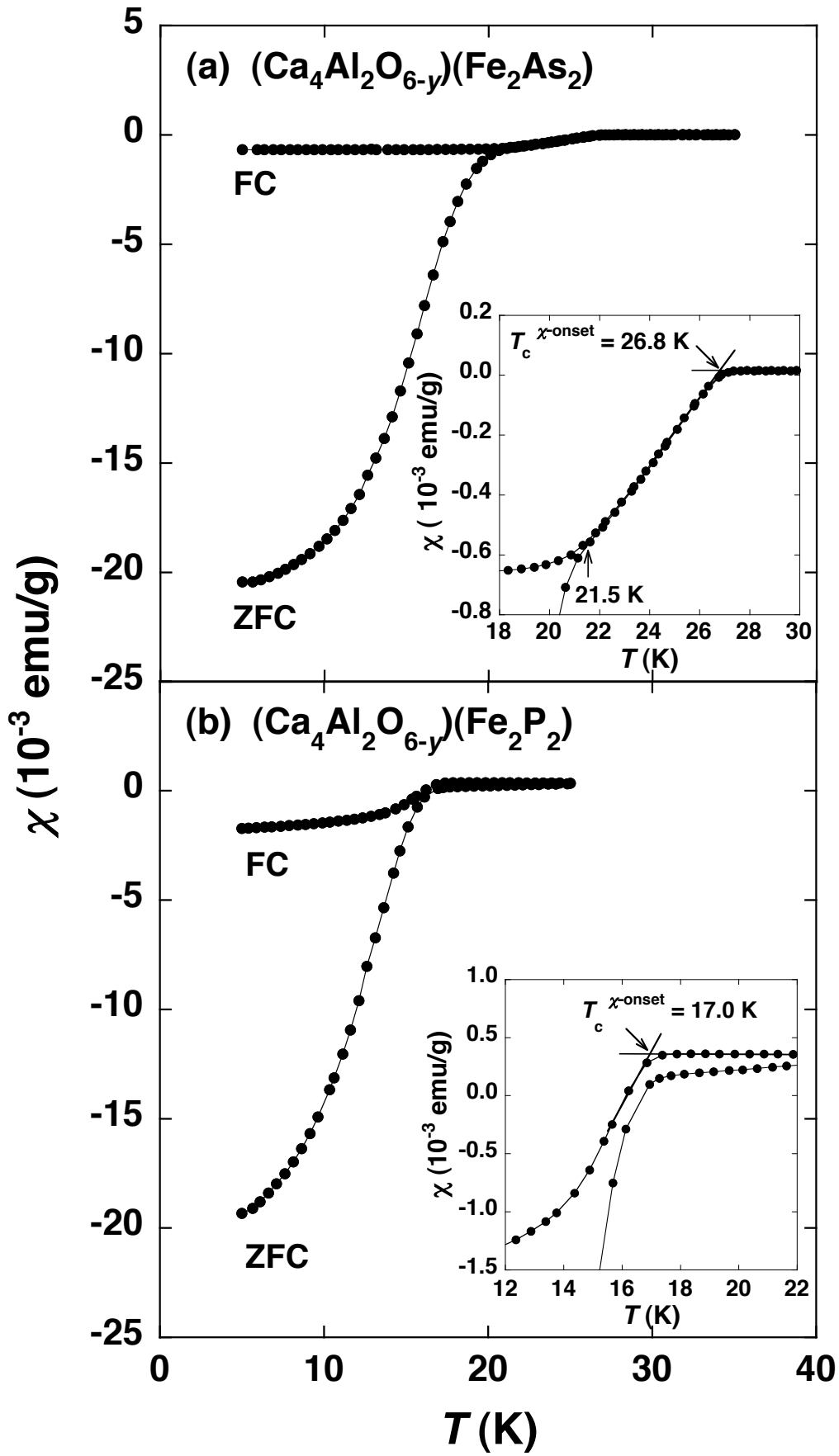


Figure 2 (a-b)

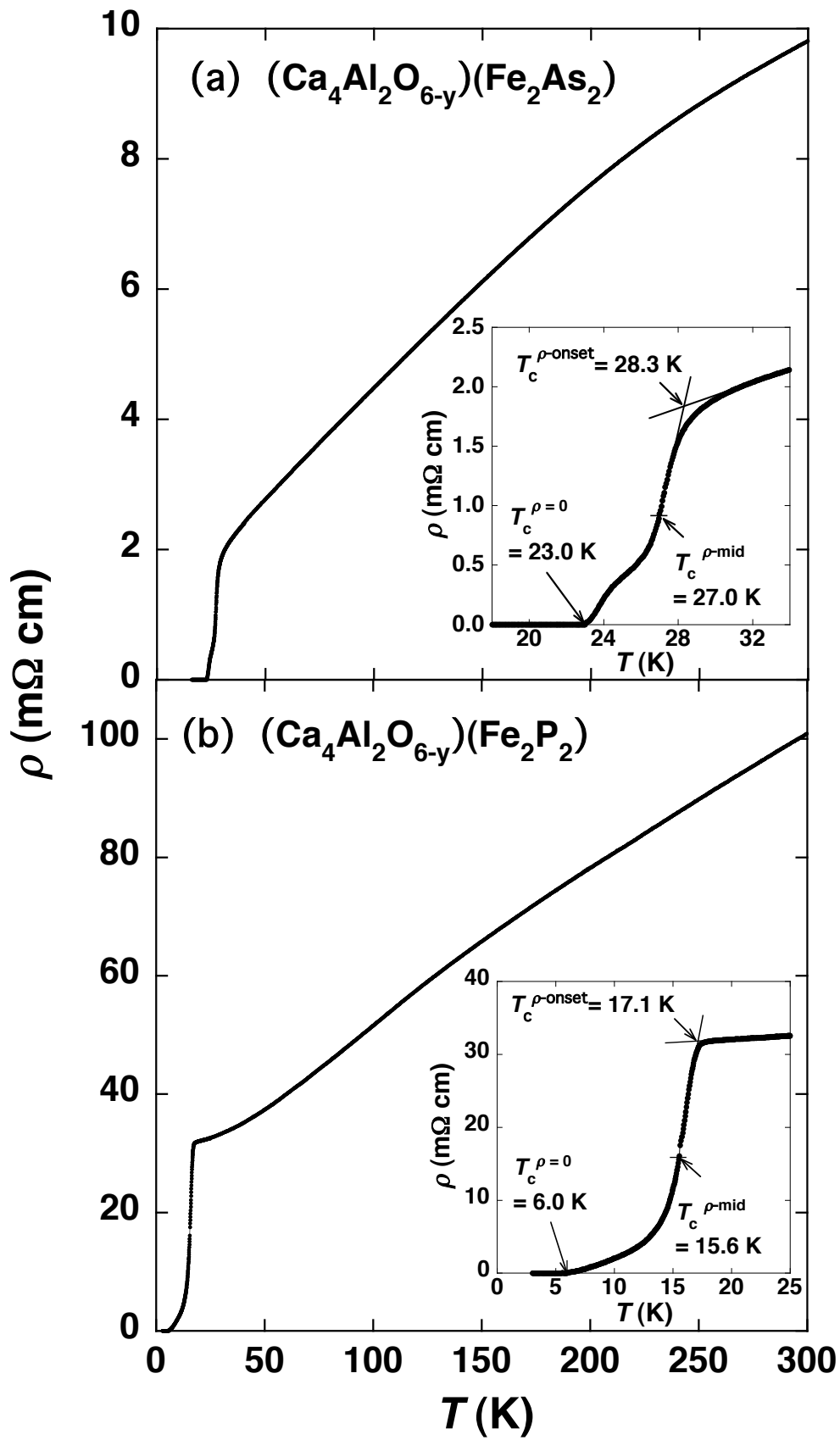


Figure 3(a-b)